

RESEARCH ARTICLE

Extensive Decoupling of Metabolic Genes in Cancer

Ed Reznik*, Chris Sander

Computational Biology Program, Memorial Sloan Kettering Cancer Center, New York, New York, United States of America

* reznike@mskcc.org



 OPEN ACCESS

Citation: Reznik E, Sander C (2015) Extensive Decoupling of Metabolic Genes in Cancer. *PLoS Comput Biol* 11(5): e1004176. doi:10.1371/journal.pcbi.1004176

Editor: Jennifer L. Reed, University of Wisconsin-Madison, UNITED STATES

Received: November 4, 2014

Accepted: February 4, 2015

Published: May 11, 2015

Copyright: © 2015 Reznik, Sander. This is an open access article distributed under the terms of the [Creative Commons Attribution License](https://creativecommons.org/licenses/by/4.0/), which permits unrestricted use, distribution, and reproduction in any medium, provided the original author and source are credited.

Data Availability Statement: All relevant data is available through the publically accessible Broad Institute Firehose, which aggregates data from the Cancer Genome Atlas.

Funding: ER and CS were supported by grants from the U.S. National Institutes of Health: Division of Biomedical Technology, Bioinformatics, and Computational Biology (P41 GM103504), National Human Genome Research Institute (U41 HG006623) and the National Cancer Institute Cancer Genome Atlas (U24 CA143840). The funders had no role in study design, data collection and analysis, decision to publish, or preparation of the manuscript.

Abstract

Tumorigenesis requires the re-organization of metabolism to support malignant proliferation. We examine how the altered metabolism of cancer cells is reflected in the rewiring of co-expression patterns among metabolic genes. Focusing on breast and clear-cell kidney tumors, we report the existence of key metabolic genes which act as hubs of differential co-expression, showing significantly different co-regulation patterns between normal and tumor states. We compare our findings to those from classical differential expression analysis, and counterintuitively observe that the extent of a gene's differential co-expression only weakly correlates with its differential expression, suggesting that the two measures probe different features of metabolism. Focusing on this discrepancy, we use changes in co-expression patterns to highlight the apparent loss of regulation by the transcription factor HNF4A in clear cell renal cell carcinoma, despite no differential expression of HNF4A. Finally, we aggregate the results of differential co-expression analysis into a Pan-Cancer analysis across seven distinct cancer types to identify pairs of metabolic genes which may be recurrently dysregulated. Among our results is a cluster of four genes, all components of the mitochondrial electron transport chain, which show significant loss of co-expression in tumor tissue, pointing to potential mitochondrial dysfunction in these tumor types.

Author Summary

The metabolism of malignant tumors is deranged. The transition from healthy to cancerous state involves, among other factors, the transcriptional coordination of genes spread throughout the cell's metabolic pathways. An examination of this multivariate regulatory effort can offer insights which may remain hidden from analyses focusing on a single gene in isolation. Such an analysis is particularly relevant for metabolic networks, whose constituent enzymes are fundamentally linked through their common utilization of a limited pool of substrates. Here, we examine the extent to which altered metabolism is reflected in the co-expression patterns of genes, shedding light on the differential regulation of metabolic genes within tumors. We study patterns of differential co-expression across metabolic pathways in both breast and kidney tumors, and integrate regulatory information to study the drivers of these changes. Among the results of our analysis is the apparent

Competing Interests: The authors have declared that no competing interests exist.

dsyregulation of genes controlled by HNF4A in clear-cell kidney tumors. Finally, by combining the results of our analyses across seven different tissues, we identify the recurrent decoupling of a set of mitochondrial genes, pointing to possible mitochondrial dysfunction in these cancers.

Introduction

All cellular events, from the transduction of signals to the translation of nucleic acids, rely on the interaction of molecular entities. Indeed, one may argue that the fundamental unit of a biological network is not its constituent components (*e.g.* proteins or genes), but rather the edges representing the interactions between them. Then, it follows that the manifestation of disease, of a deranged phenotype of this network, should be evident by observing changes in the wiring and activity of these edges.

Here, we study the interactions between pairs of genes encoding metabolic enzymes, and how these interactions change in the course of transformation of normal cells to malignant tumor. This notion of studying “interactions” is particularly important for understanding the network of coupled enzymatic reactions which constitute metabolism. It is well-known that tumors, which are under strong selection for proliferative capacity, must re-organize their metabolism in order to deliver the precursors and energy needed to grow as quickly as possible. Otto Warburg published a series of key findings highlighting a fundamental dysregulation in glycolytic metabolism in cancer, whereby cancer cells metabolized high levels of glucose to lactate [1]. Some of the earliest chemotherapies (*e.g.* methotrexate) targeted a metabolic phenotype which distinguished tumor from normal tissue. In recent years, an invigorated field has identified a number of distinct “metabolic lesions” in various tumors, including, for example, the preferential expression of PKM2 [2] and the presence of an oncometabolite, 2-hydroxyglutamate, in cells with activating IDH1 and IDH2 mutations [3].

Our use of the term “interaction” above is loose: for the purposes of our study, which focuses on the analysis of gene expression data, we say that two metabolic genes putatively interact if we observe they are co-expressed. This co-expression may occur by chance, or as a result of co-regulation by a set of common factors. Furthermore, while strong co-expression is more likely to occur between proteins which physically interact with each other, the highly connected structure of the metabolic network suggests that even genes residing in opposing corners of metabolism may be coupled to each other. Regardless of the source of co-expression, our goal is to identify regions of the metabolic network whose co-expression patterns appear fundamentally different between normal and cancerous tissue samples. Put another way, we intentionally search for cases where two genes are co-expressed in one manner in normal tissue, and then co-expressed in an entirely different manner in the tumor tissue. Our approach follows other studies employing techniques to detect so-called “differential co-expression” of genes [4–11].

Differential expression analysis is the standard method for comparing the expression patterns of genes across conditions. Aside from its ubiquitous use in research, several large-scale surveys of differential expression focusing exclusively on metabolic genes in cancer have been completed [12, 13]. In contrast, while a handful of publications have examined differential co-expression in various cancer settings (for example, [9, 14–17]), differential co-expression analysis remains largely absent in most studies of gene expression and (to our knowledge), no survey of differential co-expression among metabolic genes in cancer has been undertaken. This is, at least in part, due to the requirement for large sample sizes in order to detect statistically significant differential co-expression patterns. Here, we embark on such a large-scale analysis

Table 1. Cancer data used in this study.

Study	Number Tumor Samples	Number Normal Samples	Individual Analysis	PanCan Analysis
Breast Cancer	914	106	X	X
Clear Cell Renal Cell Carcinoma	480	71	X	X
Head and Neck Squamous Cell Carcinoma	303	37		X
Liver Cancer	103	49		X
Lung Adenocarcinoma	446	57		X
Prostate Adenocarcinoma	176	44		X
Thyroid Cancer	482	58		X
Total	2904	422		

doi:10.1371/journal.pcbi.1004176.t001

of RNA-Seq data from 3000 samples of primary tumor and adjacent normal samples from seven distinct tissues, and focus our attention squarely on the expression patterns of 1789 metabolic genes. Among our main findings is the (previously known, see [18], but potentially under-appreciated) observation that genes with strong differential co-expression patterns are not necessarily differentially expressed. A relatively large fraction of the genes we identify in our study show no substantial difference in their absolute expression between tumor and normal tissue, but nevertheless exhibit recurrent differential co-expression.

The results to be presented will encompass a variety of analyses, studying differential co-expression patterns first across two cancer types for which we have the most data available (breast and clear cell renal cell carcinomas, (KIRC)), and then expanding to include five other cancer types (lung, thyroid, prostate, liver, and head and neck), as described in Table 1. In the course of doing so, we propose two simple, but novel, analyses which integrate pathway information to assess the functional role of differentially co-expressed gene pairs. We examine the association between differential co-expression and differential expression, and identify genes which are strongly enriched for one measure but not the other. By leveraging our findings against regulatory (*i.e.* transcription factor binding) data, we identify transcription factors whose targets are highly enriched for differential co-expression. Among our findings is a previously unreported loss of co-expression between HNF4A, a transcription factor, and its regulatory targets in KIRC. Finally, we leverage the scale of our study to complete a “Pan-Cancer” analysis of differential co-expression, searching for those pairs of metabolic genes which are recurrently differentially co-expressed across multiple cancer types. Our results highlight a small group of four mitochondrial electron transport chain (ETC) genes which are recurrently differentially co-expressed, hinting at a fundamental alteration in the function of the ETC in tumors.

Methods

Data

All TCGA expression data were accessed using the Broad Institute Firehose. RSEM-normalized expression was used for the co-expression calculations. Entrez IDs of metabolic genes were extracted from the Recon2 genome scale metabolic network reconstruction [19], and used to extract the corresponding metabolic gene expression data from the TCGA datasets.

Calculation of Changes in Gene Co-expression

We begin by describing the methodology, broadly illustrated in Fig 1, to detect changes in co-expression patterns between normal and tumor samples. After obtaining RNA-Seq data, we

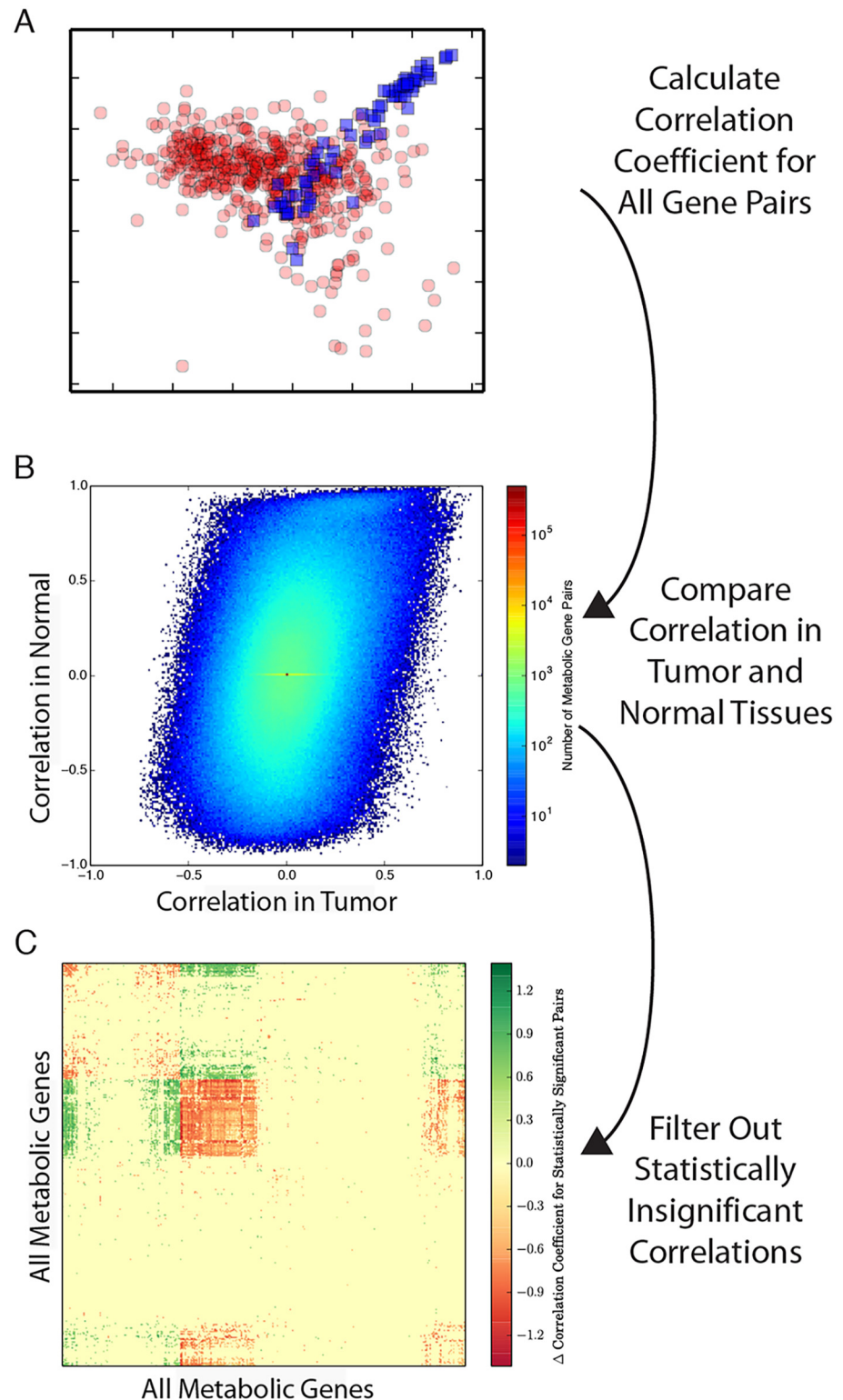


Fig 1. Outline of the method to calculate differential co-expression. (A) Calculate the co-expression for each pair of metabolic genes across tumor (red) and normal (blue) samples, respectively. (B) For each pair of genes in a given tumor type (e.g. breast), compare the Spearman correlation coefficient in tumor and normal samples. Most pairs of genes show very similar co-expression in both tumor and normal samples (reflected in the high density of points in the center of the plot). More rarely, a pair of genes will show significantly different

co-expression between normal and tumor samples (e.g. bottom right and top left corners). (C) Using the statistical methodology detailed in Eq 4, filter out insignificant differences in correlation coefficients. Retain the remaining (significant) differences in correlations in the matrix **D**. The filtered results can then be analyzed further to identify regions of metabolism enriched for differential co-expression.

doi:10.1371/journal.pcbi.1004176.g001

calculate the Spearman correlation (a non-parametric measure of the correlation of two random variables employing ranks) of each pair of genes i, j , and record the p-value p_{ij} associated with this correlation. These calculations are performed separately for tumor and normal samples. To account for multiple hypothesis testing, we apply the conservative Bonferroni correction [20], yielding corresponding adjusted p-values \hat{p} . The results of these correlation calculations are stored in two matrices, C^T and C^N (corresponding to tumor and normal samples, respectively), with entries

$$C_{ij} = \begin{cases} r_{ij}, & \text{if } \hat{p}_{ij} < \tau \\ 0, & \text{otherwise} \end{cases} \quad (1)$$

Here, τ is a significance threshold for our Bonferroni-corrected p-values. Throughout the manuscript unless otherwise stated, we employ a threshold $\tau = 1 \times 10^{-2}$.

Our goal is to identify significant differences between the strength of co-expression (as quantified by the correlation coefficients) in tumor and normal samples. Such a comparison of sample correlation coefficients must be done with care. In fact, the difference between two correlation coefficients is not sufficient information to determine how often such a difference would appear by chance. We offer an example to illustrate this phenomenon. Very small correlation coefficients (say, $r_1 = 0.1, r_2 = -0.1$) may appear in random, uncorrelated data simply by chance. In this case, the difference between the two correlation coefficients ($r_1 - r_2 = 0.2$) should be categorized as statistically insignificant because it is quite likely to happen by chance. On the other hand, the same difference for two very large correlation coefficients (say, $r_1 = 0.99, r_2 = 0.79$) appears less likely to happen by chance; instead, this difference is more likely to arise via the corruption of a nearly perfect correlation by a confounding factor or noise.

The basis of this intuition is that very large correlation coefficients are observed quite rarely by chance. More importantly, the variance of the correlation coefficient estimated from the data (referred to as the *sample* correlation coefficient, r) depends on the value of the *true* correlation coefficient underlying the data (referred to as the *population* correlation coefficient, ρ). In particular, the variance of sample correlation coefficient is approximately [21, 22]

$$\text{Var}(r) \propto (1 - \rho^2)^2$$

Thus, as the population correlation coefficient tends to ± 1 , the variance of the sample correlation coefficient asymptotically approaches zero. This dependence of the variance of r on ρ itself makes it very difficult to carry out hypothesis tests comparing two sample correlation coefficients. A standard method for testing for a difference between correlation coefficients is to employ a transformation to *stabilize* the variances, making them independent of ρ . Here, we use the Fisher r to z transformation:

$$z = \frac{1}{2} \log \left(\frac{1+r}{1-r} \right). \quad (2)$$

The change of variables in Eq (2) is well-known, and has been used in prior work on differential co-expression [7]. When applied to data drawn from a bivariate normal distribution, this

transformation yields a quantity which is approximately normally distributed with variance $\sigma^2 = \frac{1}{\sqrt{N-3}}$ independent of the population mean, with N equal to the size of the population. By applying this transformation to our measured correlation coefficients in normal tissue and tumor samples, we are able to apply a Z-test to determine if the correlation coefficients r_{ij}^T and r_{ij}^N are significantly different. In particular, the quantity (3), which measures the difference between the two transformed correlation coefficients, is approximately normally distributed with mean zero and variance one:

$$\Delta z_{ij} = \frac{z_T - z_N}{\sqrt{\frac{1}{N_T-3} + \frac{1}{N_N-3}}}, \tag{3}$$

where N_T is the number of tumor samples, N_N is the number of normal samples, z_T is the Fisher-transformed tumor sample correlation coefficient, and z_N is the Fisher-transformed normal sample correlation coefficient. Python code for the differential co-expression test is included in [S1 Code](#). Thus, we can associate p-values p_{ij}^z with the Z-test in (3) for each pair of genes i, j . After again correcting p^z for multiple hypothesis testing using the Bonferonni correction, we stored the results of our calculations in a matrix \mathbf{D} with entries

$$D_{ij} = \begin{cases} \Delta r_{ij}, & \text{if } \hat{p}_{ij}^z < \tau \text{ and } (\hat{p}_{ij}^T < \tau \text{ or } \hat{p}_{ij}^N < \tau) \\ 0, & \text{otherwise} \end{cases} \tag{4}$$

where \hat{p}_{ij}^z is the Bonferonni adjusted value of p_{ij}^z . The entries of the matrix \mathbf{D} correspond to the change in gene co-expression between tumor and normal samples, and will be our main object of study. We emphasize one final, but important, feature of [Eq 4](#): an entry of \mathbf{D} is nonzero if and only if that gene pair shows *both* (1) a significant change in co-expression between tumor and normal samples, *and* (2) the genes were co-expressed at a statistically significant level in tumor or normal samples (or both). This ensures that those gene pairs which we call differentially co-expressed are also co-expressed at a statistically significant level in at least one group of samples.

Pathway Scores for Differential Co-expression Breast and Kidney Cancers

We assigned each gene in our study to one or more pathways using the subsystem assignments in the Recon2 human metabolic reconstruction [19]. Then, for each TCGA study, we calculated a score for each pathway i , E_i , using:

$$E_i = \sum_{j \in P_i} S_j^0, \tag{5}$$

where P_i is the set of all genes in pathway i . Thus, E_i counts the total number of dysregulations for all genes in pathway i . We then divided each E_i by the number of genes in pathway i to obtain a normalized pathway score \hat{E}_i . Thus, \hat{E}_i quantifies the differential co-expression of all genes in a pathway, averaged over the number of genes in that pathway. We excluded from our analysis pathways composed of fewer than five genes.

Tests for Enrichment of Transcription Factor Targets

We obtained data on transcription factor targets from the Broad Institute’s MSigDB website [23].

Assuming that a particular regulatory factor has m targets, we calculate the total number of differential co-expression edges in the sub-network composed of only these m gene targets. In this subnetwork, there are $t = \binom{m}{2} = \frac{m \times (m-1)}{2}$ total possible edges. If we see e edges in the true subnetwork, we can calculate the probability that these edges would appear by chance. Given that the probability of a random “differential co-expression edge” in the network is p (e.g. for a Bonferonni-corrected p-value threshold of 1×10^{-2} for detecting differential co-expression, $p \approx 8 \times 10^{-3}$), the probability of seeing at least e edges by chance is

$$P = \sum_{i=e}^t \binom{t}{i} p^i (t-i)^{1-p} \tag{6}$$

A Bonferonni correction is then applied to the vector of p-values for all transcription factor motifs.

Results

Differential Co-expression in Tumor Samples

With our analytical framework established, our first aim was to assess how pervasive differential co-expression was among metabolic genes in cancer samples. We used the Recon2 human metabolic network reconstruction [19] to identify metabolic genes, and extracted expression corresponding to these genes from the TCGA datasets. We applied the differential co-expression analysis described above to two TCGA studies (breast, BRCA; and clear cell renal cell carcinoma, KIRC) with large numbers of both tumor and normal RNA-Seq samples (106 and 71 normal samples, 914 and 480 primary tumor samples, respectively). Using the list of metabolic genes from Recon2, we were able to extract data for 1,789 unique metabolic genes. We used a strict Bonferonni corrected p-value threshold of 1×10^{-2} to identify pairs of genes which we called differentially co-expressed. Across the total number of pairs of metabolic genes in our dataset (approximately $(2 \times 10^3)^2/2 = 2 \times 10^6$ distinct pairs), we calculated (for each of the two studies) that approximately 2.5 percent of gene pairs were differentially co-expressed. The top differentially co-expressed gene pairs are reported in Tables 2 and 3.

To independently test the extent of differential co-expression in our data, we followed the protocol presented in [17] and completed a permutation test to assess how frequently we

Table 2. Top differentially co-expressed genes in BRCA.

Entrez	HUGO	S_i	S_i^0	S_i^{Cat}	S_i^{Comp}
38	ACAT1	11731.9	516	11	0
5264	PHYH	13080.2	512	3	0
10449	ACAA2	10819.4	508	12	0
9588	PRDX6	10983.9	506	2	0
4259	MGST3	9211.37	494	1	0
7360	UGP2	9882.05	492	0	0
847	CAT	9462.16	490	3	1
48	ACO1	11005.9	484	3	0
7371	UCK2	6024.4	483	0	0

doi:10.1371/journal.pcbi.1004176.t002

Table 3. Top differentially co-expressed genes in KIRC.

Entrez	HUGO	S_i	S_i^0	S_i^{Cat}	S_i^{Comp}
29968	PSAT1	13719.8	492	0	0
10846	PDE10A	11676.9	474	3	0
6482	ST3GAL1	13591.9	466	0	0
1594	CYP27B1	12064.4	465	0	0
65010	SLC26A6	10902.9	451	0	0
64849	SLC13A3	15016.4	445	0	0
64077	LHPP	7200.28	444	2	0
205	AK4	9709.72	443	0	0
54682	MANSC1	9081.81	440	0	0

doi:10.1371/journal.pcbi.1004176.t003

would expect the observed changes in correlation coefficients by chance (S1 Fig). In this analysis, we shuffled the labels (e.g. tumor or normal) of all samples, and calculated the difference in correlation coefficients and transformed correlation coefficients in the new, permuted data. This process was repeated 10000 times, and the results aggregated to form a distribution. Inspection of the results confirmed that for a large number of gene pairs, the differences in correlation coefficients were larger in the real data than in the permuted data (S1 Fig). Although it was computationally intractable to complete enough permutations of the data to generate robust p-values (because of the large correction for multiple hypothesis testing), we nevertheless found that 12% of gene pairs showed a higher difference in both (1) tumor and normal correlation coefficients and (2) transformed correlation coefficients than in any of the 10000 permuted data sets. These findings supported our observation of extensive differential co-expression in metabolic genes.

Naturally, we were interested in identifying those genes which were enriched for membership in differentially co-expressed gene pairs. To find these genes, we calculated two “scores” for each gene:

1. S_i^0 , the number of differentially co-expressed gene pairs which gene i participates in
2. $S_i = -\sum_{j:\hat{p}_{ij}^z < \tau} \ln(\hat{p}_{ij}^z)$, a weighted sum of the number of differentially co-expressed pairs gene i participates in

The score S , based on Fisher’s method for combining p-values from independent statistical tests [24], accounted for both the frequency of a gene’s membership in differentially co-expressed pairs, as well as the confidence with which we could claim the gene pair was differentially co-expressed (i.e. by the magnitude of \hat{p}_{ij}^z). It is important to note that each test of differential co-expression in our dataset is not independent, so we cannot use S as a formal test statistic. However, its use as a measure of the recurrence and magnitude of a gene’s overall differential co-expression is nevertheless useful.

In breast cancer, the top-ranked gene was ACAT1 (Acetyl-CoA acetyltransferase, not be confused with the enzyme acyl-Coenzyme A: cholesterol acyltransferase 1, which is encoded by the gene SOAT1). The enzyme translated from ACAT1 catalyzes the formation of acetoacetyl-CoA, which along with acetyl-CoA is the precursor to 3-hydroxy-3-methylglutaryl-CoA. These two metabolites lie at the beginning of the mevalonate pathway, which generates precursors for cholesterol and steroid biosynthesis. Intriguingly, Freed-Pastor and colleagues [25] recently reported that upregulation of the mevalonate pathway is sufficient and necessary for mutant p53

to have phenotypic effects on cell architecture in mammary tissue. Overexpression of various genes in the mevalonate pathway has also been shown to associate with poor prognosis in breast cancer [26]. Interestingly, ACAT1 is differentially coexpressed with 11 genes for which it is a catalytic partner: ACAA2, DLD, MLYCD, HADHB, HADH, OXCT1, PCCA, PDHA1, PDHB, and ACSS1. A plot of the differences in the correlation of these genes with ACAT1 is in [S6 Fig](#). In many cases, the co-expression patterns show remarkably tight correlations in normal tissue, and these correlations are partially or completely eroded in the tumor samples. Functionally, many of these genes are part of the terminal reactions in glycolysis, lipid biosynthesis and fatty acid oxidation. This loss of co-expression suggests that the flux generated by these pathways is no longer coupled to the flux through ACAT1 in tumor cells.

For KIRC, the highest-scoring differentially co-expressed gene was PSAT1 (phosphoserine aminotransferase 1), a key enzyme in the serine biosynthesis pathway which has already been associated with breast and colorectal cancers before [27, 28], but has not yet been associated with kidney cancer. PSAT1 was differentially co-expressed with 492 other metabolic genes in the dataset, with the strongest signals coming from genes like GATM (glycine aminotransferase), GBA3 (a beta-glucosidase), and SLC10A2 (a bile transporter) ([S4 Fig](#)). Because nearly all of the strongest signals came from loss of positive correlation in normal samples, we further identified those genes with which PSAT1 was more strongly co-expressed in tumor samples than in normal samples ([S5 Fig](#)). These genes included several galactosidases (GLA, GLB1), glycogen phosphorylase (PYGB), and SLC35A2, which transfers nucleotide sugars into the Golgi body for the purposes of glycosylation. Neither the substrates (3-phosphonoxypyruvate, glutamate) nor the products (phosphoserine, 2-oxoglutarate) of PSAT1 participate in the glycogenolysis pathway, suggesting that the positive correlation between PSAT1 and glycogen breakdown in tumors may be the result of indirect couplings. In particular, it is possible that the overexpression of glycogen phosphorylase may liberate carbon units to be shunted from glycolysis into the serine biosynthesis pathway through PSAT1, as well as into the Golgi body for glycosylation in tumor cells.

Following our analysis of PSAT1, we reasoned that a particularly interesting set of genes were those showing a higher degree of co-expression (as quantified by the magnitude of the Spearman correlation coefficient) in tumor samples relative to normal samples. For both BRCA and KIRC, we isolated pairs of genes exhibiting this property, and scored each metabolic gene based on how many such interactions it participated in. Interestingly, in both studies the highest-scoring gene was associated with the metabolism of lipids. In KIRC, the highest scoring gene was mevalonate kinase, MVK, a key gene in the cholesterol pathway described above for BRCA. In breast tissue, the highest scoring gene was LIPG, an endothelial lipase which catalyzes the hydrolysis of lipids. The products of this hydrolysis can then be used for the production of signaling lipids as well as cell membrane components.

Breast and Kidney Cancers Show Distinct Co-expression Patterns

We decided to investigate more comprehensively whether differential co-expression patterns were similar between BRCA and KIRC. To probe whether common, “global” patterns of differential co-expression existed between the two studies, we completed a principal components analysis (PCA, [Fig 1A](#)). We assembled a concatenated differential co-expression matrix:

$$D_C = \begin{bmatrix} D_{BRCA} \\ D_{KIRC} \end{bmatrix} \quad (7)$$

with dimension $2m \times m$, where m is the number of genes under study. For a given index $i < m$, row i corresponded to the differential co-expression pattern of that gene in BRCA, while row m

$+i$ corresponded to the differential co-expression pattern in KIRC. Thus, each column of D_C corresponded to a metabolic gene, and stored the differential co-expression of that gene with all other metabolic genes in both breast and kidney studies.

Our expectation was that PCA would identify patterns of differential co-expression which breast and kidney cancers might share in common. Instead, we found that genes in the two studies displayed completely distinct patterns of differential co-expression (Fig 2A). While a large portion of the variance in the data was captured by the first two principal components (33 and 19 percent of the total variance in the data, respectively), most genes from breast cancer had nearly no loading on component 2, while most genes from kidney cancer had nearly no loading on component 1. The result was the cross pattern evident in Fig 2A.

Despite the results above, we still found a small positive correlation (Spearman ρ 0.28, p -value $< 1e-30$, Fig 2C) between differential co-expression in the two cancer types, suggesting that many genes showed high (or low) levels of differential co-expression in both studies. In general, most genes participated in relatively few differential co-expression interactions, while a small subset of “hub” genes participated in hundreds (Fig 2C, histograms). A particularly interesting example was ASS1, an enzyme involved in arginine synthesis and the synthesis of nitric oxide and polyamines. It is known that several tumor types exhibit an arginine auxotrophy phenotype, and are unable to proliferate in the absence of arginine [29]. Intriguingly, Qiu and colleagues recently reported the killing of triple-negative breast cancer cell lines under arginine deprivation, identifying it as a lucrative therapeutic target [30]. It is not clear from our analysis whether differential co-expression of ASS1 is associated with such a vulnerability, but its recurrent differential co-expression in both studies suggests that its activity may play an important role in malignancy.

The results of the PCA analysis above reflected the large number of cases of high differential co-expression in one tumor type, but none in the other. We explicitly identified such cases by calculating the mean and standard deviation of S^0 (the number of differentially co-expressed gene pairs a gene participates in) for each study. We then searched for genes with S^0 greater than two standard deviations above the mean S^0 in one study, but with $S^0 = 0$ in the other study (Fig 2C, blue and green points). KIRC-specific differentially co-expressed genes were highly enriched for SLC and ABC transporters. A particularly interesting kidney-specific gene was DPEP1 (a dipeptidase) in light of the recently observation of elevated dipeptide levels in a subset of clear cell renal carcinoma tumors (manuscript in preparation). In contrast, BRCA-specific genes included CDO1 (cysteine dioxygenase Type 1, whose inactivation was recently reported to contribute to survival and drug resistance in breast cancer [31]) and a number of genes involved in glycerolipid/lipid biosynthesis and associated with malignancy in breast cancer (GPAM [32] and MGLL [33]).

We also made special note of those pairs of differentially co-expressed genes which took part in a known, previously reported biological interaction. To do so, we extracted from the Pathway Commons database [34] a list of pairs of genes known to interact in either of two ways: 1) through the formation of a complex with each other (“In-Complex-With” interactions), and 2) through the production of a metabolite by the enzyme encoded by one gene in the pair, and subsequent use of that metabolite as a substrate for the enzyme encoded by the other gene in the pair (“Catalysis-Precedes” interactions) [35]. We then identified which pairs of differentially co-expressed genes participated in either of these kinds of interactions. These results were summarized in two additional gene-level statistics, S_i^{Comp} and S_i^{Cat} , indicating the number of differentially co-expressed catalysis-precedes and in-complex-with interactions, respectively, a gene i participates in.

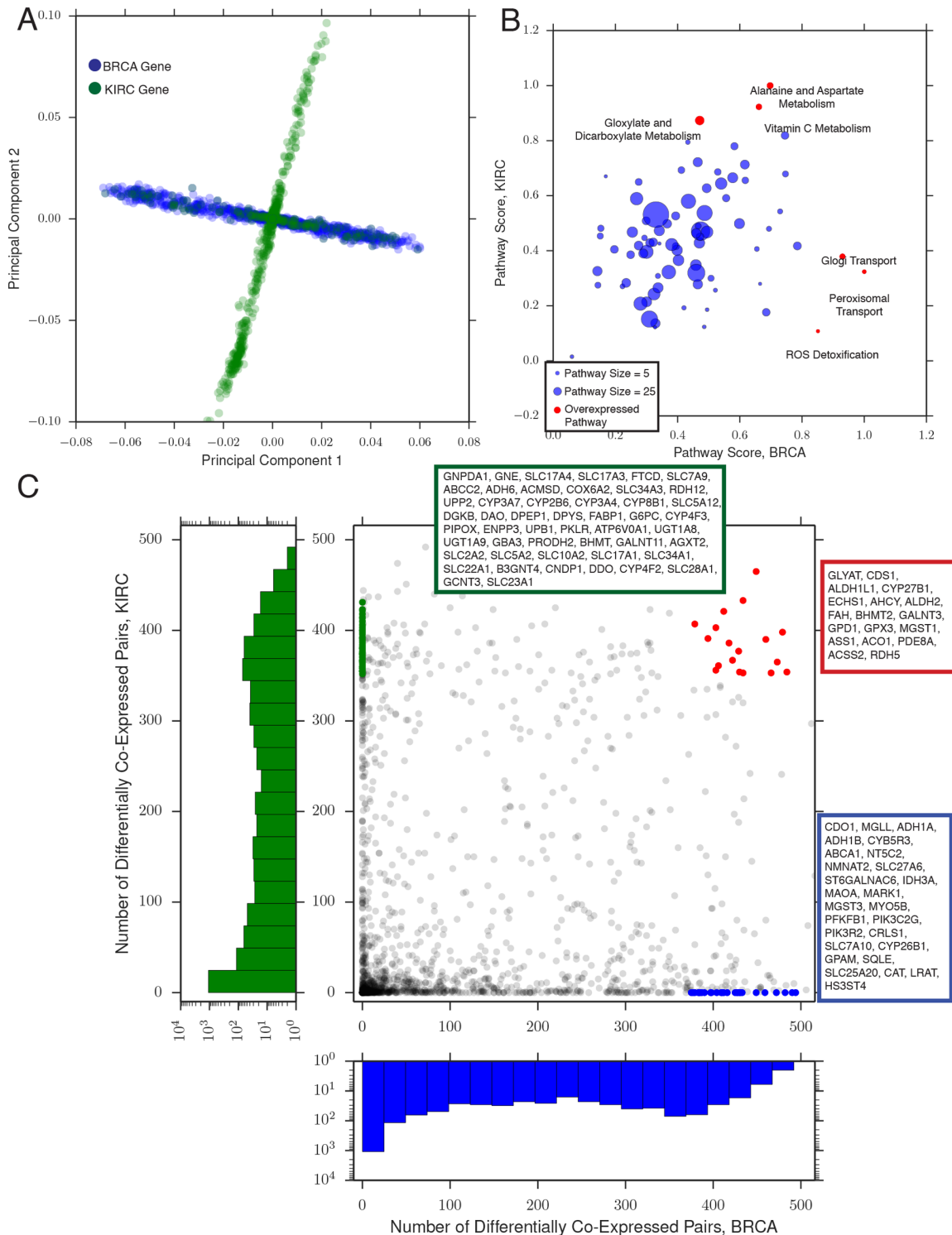


Fig 2. (A) Principal components analysis (PCA) for the breast (green) and kidney (blue) differential co-expression data. Each dot represents one gene. Data from kidney tumors exhibits variation mostly along the first principal component, while data from breast tumors varies mostly along the second, suggesting that the dominant modes of variation in the two tumor types are distinct from each other. **(B)** Differential co-expression pathway analysis. Each axis denotes the enrichment score for a pathway in breast or kidney tumors, respectively. Red dots indicate significantly over- or under-enriched pathways. **(C)** A comparison of the score S^0 in breast and kidney tumors. Each dot is a single gene. A number of genes (blue and green dots and inset boxes) show extensive differential co-expression in one tumor type, but none in the other. Other genes (red dots and inset box) are highly differentially co-expressed in both.

doi:10.1371/journal.pcbi.1004176.g002

We compared the incidence of differential co-expression among pairs of genes participating in the binary interactions described above, to genes not participating in such interactions. To do so, we compared the distribution of transformed correlation coefficients (defined in 3) for the two groups of genes. We found a striking drop in co-expression among metabolic genes participating in a common molecular complex, an effect that was evident in both BRCA and KIRC (t-test, p-value $< 1 \times 10^{-200}$ BRCA, $< 1 \times 10^{-75}$ KIRC, S2 Fig, S3 Fig). A much weaker, but statistically significant, effect was also observed for catalytically adjacent genes (t-test, p-value $< 1 \times 10^{-18}$ BRCA, .0002 KIRC). Together, the results suggest a disruption of metabolic complexes in these two cancers. A more detailed future investigation is required to determine if this phenomenon is limited to metabolism, or is evident across all molecular complexes.

Finally, we analyzed the pattern of differential co-expression across metabolic pathways, as annotated in the Recon2 metabolic network [19] (see Methods). The results of our analysis are highlighted in Fig 2B, where we compared the score of each pathway in BRCA and KIRC, respectively. In breast cancer, among the most enriched pathways is peroxisomal transport genes, including the peroxisomal transporters ABCD1, ABCD2, and ABCD3, which transport fatty acids and acyl-CoAs and have been shown to be markers of tumor progression and response to therapy [36]. Notably, genes in the vitamin C pathway were enriched for differential co-expression in both cancers, possibly as an indirect consequence of high oxidative stress within the tumors.

Differential Expression Sheds Little Light On Differential Co-expression

A common first step in the analysis of gene expression data across samples is the identification of differentially expressed transcripts. The underlying rationale behind differential expression analysis of metabolic genes is intuitive: higher expression of genes in one condition over another suggests a difference in metabolic flux through those sets of genes. In this study, we are more concerned with the coupling of genes together: since metabolic genes are components of a network, different co-expression patterns may lead to differences in metabolic flux. Naturally, one may ask whether the two measures are in agreement; in other words, do genes which are up- or down-regulated in tumor (compared to normal tissue) also exhibit large differences in co-expression patterns in tumor (compared to normal) samples?

To explicitly test the connection between differential co-expression and differential expression, we compared the two measures for metabolic genes in BRCA and KIRC (Fig 3). We assessed differential expression using the limma voom package [37]. We found that the magnitude of differential expression (as quantified by the \log_2 ratio of tumor to normal expression) was weakly associated with the frequency of differential co-expression of a gene (BRCA, Spearman ρ 0.21, p-value 3×10^{-17} ; KIRC, Spearman ρ 0.11, p-value 4×10^{-6}). In spite of this weak association, many of the most differentially expressed genes were members of very few dysregulated gene pairs, and conversely many genes which exhibited no substantial change in expression levels nevertheless were found to be frequent members of dysregulated gene pairs (S7 Fig).

The most intriguing observation we made was that a number of genes showed no measurable change in absolute expression levels, but nevertheless were among the most differentially co-expressed genes in the entire dataset (green dots, Fig 3). To find exceptional cases like these, we identified genes with S^0 greater than 2 standard deviations above the mean S^0 for the study, but with an absolute \log_2 ratio of less than 0.2. For breast cancer, these genes included PLOD2 (procollagen lysyl hydroxylase 2 [38], recently reported to be essential for hypoxia-induced breast cancer metastasis), and LDHA, a key enzyme in the terminal end of glycolysis. In KIRC,

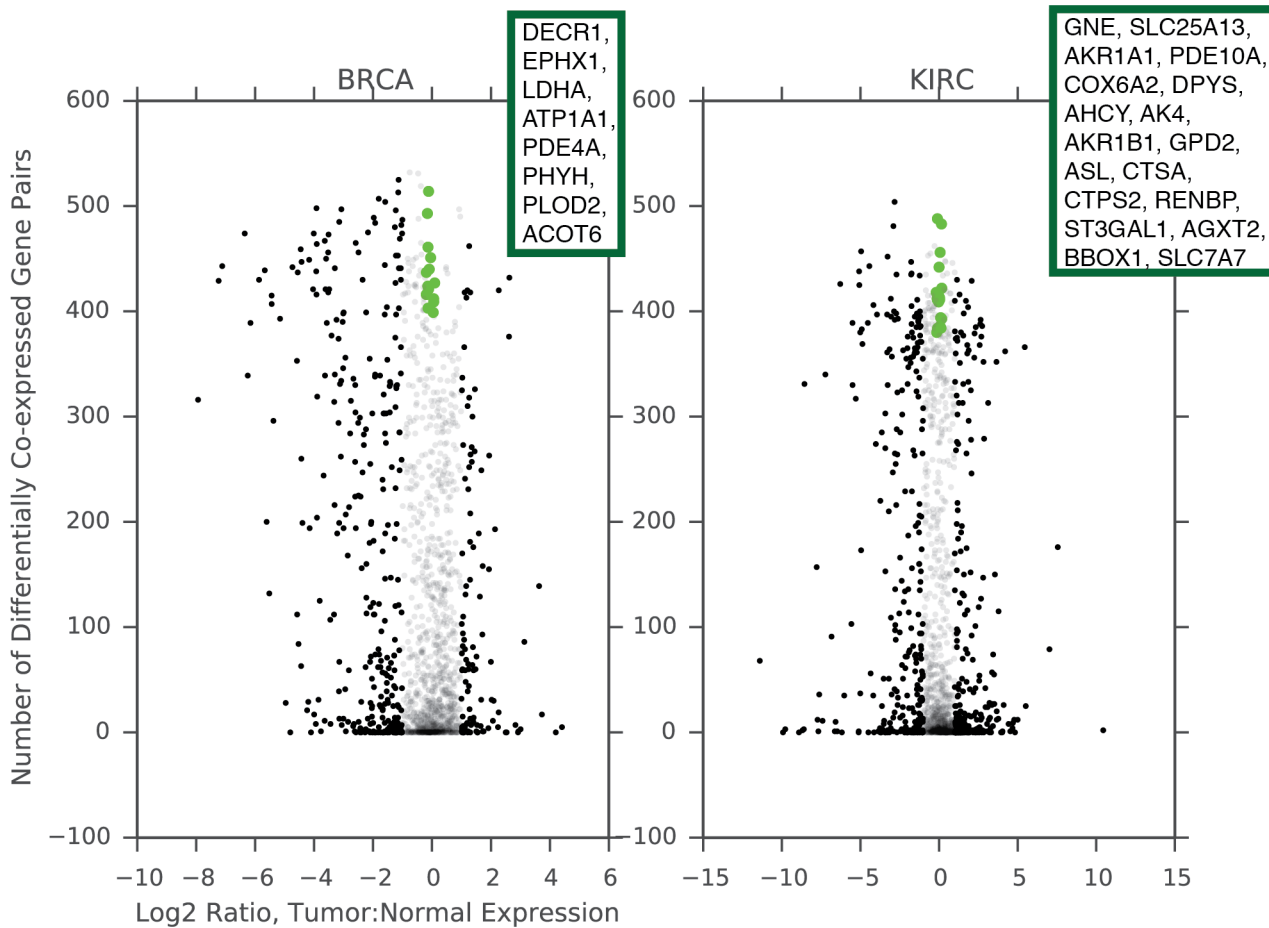


Fig 3. Differential expression and differential co-expression are only weakly correlated. Green dots, detailed in insets, indicate genes with high differential co-expression score S_i^0 (> 2 standard deviations above the mean S_i^0) but very small absolute fold ratio (< 0.1). Black dots indicate a gene is differentially expressed with corrected p-value less than 0.01 and absolute fold \log_2 fold ratio greater than 1. Transparent dots correspond to genes which are not differentially expressed.

doi:10.1371/journal.pcbi.1004176.g003

several of the genes we identified (RENPB, GNE, and CTSA) were members of the glycoprotein sialylation pathway, which has also been associated with metastasis [39].

The presence of genes with exceptionally high differential co-expression and essentially no differential expression (and the converse) deserves further discussion. It is possible that, depending on how the activity of a metabolic pathway is modulated, either differential expression or differential co-expression may be a more suitable technique for identifying such modulation. In one case, a gene may change in synchrony with its regulatory partners; that is, regardless of whether the gene is over- or under-expressed relative to normal tissue, it exhibits precisely the same co-expression patterns. Such an effect may be observed, for example, following the over-expression of a transcription factor common to all the genes in a co-expressed cluster. As we suggested earlier, synchronous regulation of a metabolic pathway may serve as a mechanism for increasing flux through the pathway, and would be detected through standard differential expression analysis. In contrast, a gene's expression may correlate with different sets of genes in different conditions. In our case, the control over expression wielded by one transcription factor in normal tissue TF_N would be ceded to a different transcription factor in tumor tissue

TF_T . The consequence is that the gene of interest is co-expressed with a completely distinct set of genes under the control of TF_T . The differential co-expression of such a gene provides indirect evidence that the source or destination of metabolic flux through the enzyme encoded by this gene may be changing from normal to tumor tissues.

Signatures of Regulation in Differential Co-expression Patterns

As alluded to above, the expression of genes is fundamentally orchestrated by regulatory factors such as transcription factors and microRNAs. Thus, the differential co-expression patterns we observe are likely due, at least in part, to differential regulatory activity by these molecules. Inspired by prior work linking transcription factors with observations of differential co-expression [18, 40], we examined our differential co-expression networks for an enrichment of targets associated with particular transcription factor motifs annotated in MSigDB [23]. To detect such enrichment, we isolated metabolic genes which were reported targets of a particular transcription factor. Then, we applied a binomial test (see Methods) to quantitatively assess whether the number of differential co-expression edges existing between only these target genes was higher than would be expected by chance. We used only highly significant differentially co-expressed edges, with a p-value threshold of 1×10^{-10} .

Among the 556 transcription factor motifs we examined, only a handful were enriched in either kidney or breast cancer. In breast cancer, 21 transcription factors were identified as enriched in differentially co-expressed gene targets. The most enriched transcription factors (reported in Table 4) included SP1, NFAT, and ERR1. Several of these transcription factors have already been reported to play important roles in breast cancer throughout the literature. SP1 is known to be involved in cell proliferation, apoptosis, and cell differentiation and transformation, and has been reported as a prognostic marker for breast cancer [41, 42]. Both NFAT and SP1 have been shown to induce invasion of breast tissue via the transcriptional modulation of downstream genes [42, 43]. Perhaps most interesting is the identification of ERR1 (estrogen-related-receptor 1, also known as $ERR-\alpha$), an orphan receptor known to interact with PGC1- α to regulate a number of metabolism-related genes. $ERR-\alpha$ is regulated by ErbB2/Her2 signaling [44], and is associated with poor outcomes in breast cancer patients [45].

For kidney cancer, the pattern was far more unanimous: several of the most enriched transcription factor target sites were targets of HNF4A (Table 5). Out of the 15 transcription factors

Table 4. Transcription factors most enriched for differential co-expression targets in BRCA.

MSigDB Transcription Factor Motif	P-Value
SP1-Q6	2×10^{-22}
HNF4-01	9×10^{-16}
NFAT-Q4-01	3×10^{-13}
FREAC2-01	1×10^{-11}
ETS2-B	2×10^{-8}
AACTTT-UNKNOWN	6×10^{-8}
ERR1-Q2	8×10^{-8}
YNGTTNNNATT-UNKNOWN	5×10^{-7}
HFH8-01	8×10^{-7}
CTTTAAR-UNKNOWN	4×10^{-6}

doi:10.1371/journal.pcbi.1004176.t004

Table 5. Transcription factors most enriched for differential co-expression targets in KIRC.

MSigDB Transcription Factor Motif	P-Value
LEF1-Q2	4×10^{-45}
HNF4-Q6	2×10^{-31}
HNF4-01	7×10^{-30}
HNF4ALPHA-Q6	7×10^{-24}
HNF4-DR1-Q3	1×10^{-13}
HNF4-01-B	4×10^{-10}
COUP-01	4×10^{-8}
PPAR-DR1-Q2	6×10^{-7}
PAX4-02	6×10^{-5}
IK3-01	0.0002

doi:10.1371/journal.pcbi.1004176.t005

identified as enriched for differentially co-expressed gene targets, 5 were associated with HNF4. HNF4A is known to control cell proliferation in kidney cancer cell lines, and regulates a number of well-known cancer-associated genes to do so (e.g. CDKN1A and TGFA) [46–48]. Interestingly, HNF4A (one of the two isomers of HNF4, which was most enriched for differential co-expression targets) shows no clear differential expression pattern between KIRC tumor samples and adjacent normal tissue samples (Fig 4A), but does seem to exhibit more variation in tumor samples than in normal samples.

On the other hand, the co-expression of HNF4A and its metabolic gene targets is markedly different in normal and tumor samples (Fig 4B). A number of these genes (including PIK3R3, a member of the PI3K pathway, and PKLR, an isoform of pyruvate kinase) showed exceptionally strong co-expression with HNF4A in normal samples, only to have this co-expression abrogated in tumor samples (S8 Fig). Similarly, many of the strong co-expression patterns existent between the targets of HNF4A and HNF4A itself in normal samples were also abrogated in tumor samples (Fig 4B). Together, these findings suggest that the regulatory program associated with HNF4A in normal tissue is disrupted in tumor tissue, a hypothesis in line with previous findings implicating its dysregulation with increased cell proliferation [46]. Given its high score in our enrichment analysis, we tested whether the expression of HNF4A was associated with patient survival in the TCGA data. After stratifying patients into groups with high and low expression (relative to the mean expression of HNF4A in the tumor samples), we found that low HNF4A expression is associated with shorter survival in KIRC patients (Fig 4D, log-rank p-value 0.007).

Taken together, our observations above suggest that HNF4A’s control over the expression of its targets changes in at least a subset of clear cell kidney tumors when compared to normal kidney tissue. It is possible that this loss of control occurs via under-expression of HNF4A itself. It is also possible that (as we proposed in the prior section) other transcription factors exert a more dominant control over HNF4A’s targets. In either case, this leads to the loss of co-expression among HNF4A’s targets, and between HNF4A itself and its targets.

PanCan Patterns of Differential Co-expression

This final section of our work strikes out into more difficult territory: we ask whether some patterns of differential co-expression may exist throughout different cancer types, regardless of their tissue of origin. While we have found a number of apparently dysregulated metabolic genes specific (and in some cases, common) to breast and clear cell renal cell carcinoma

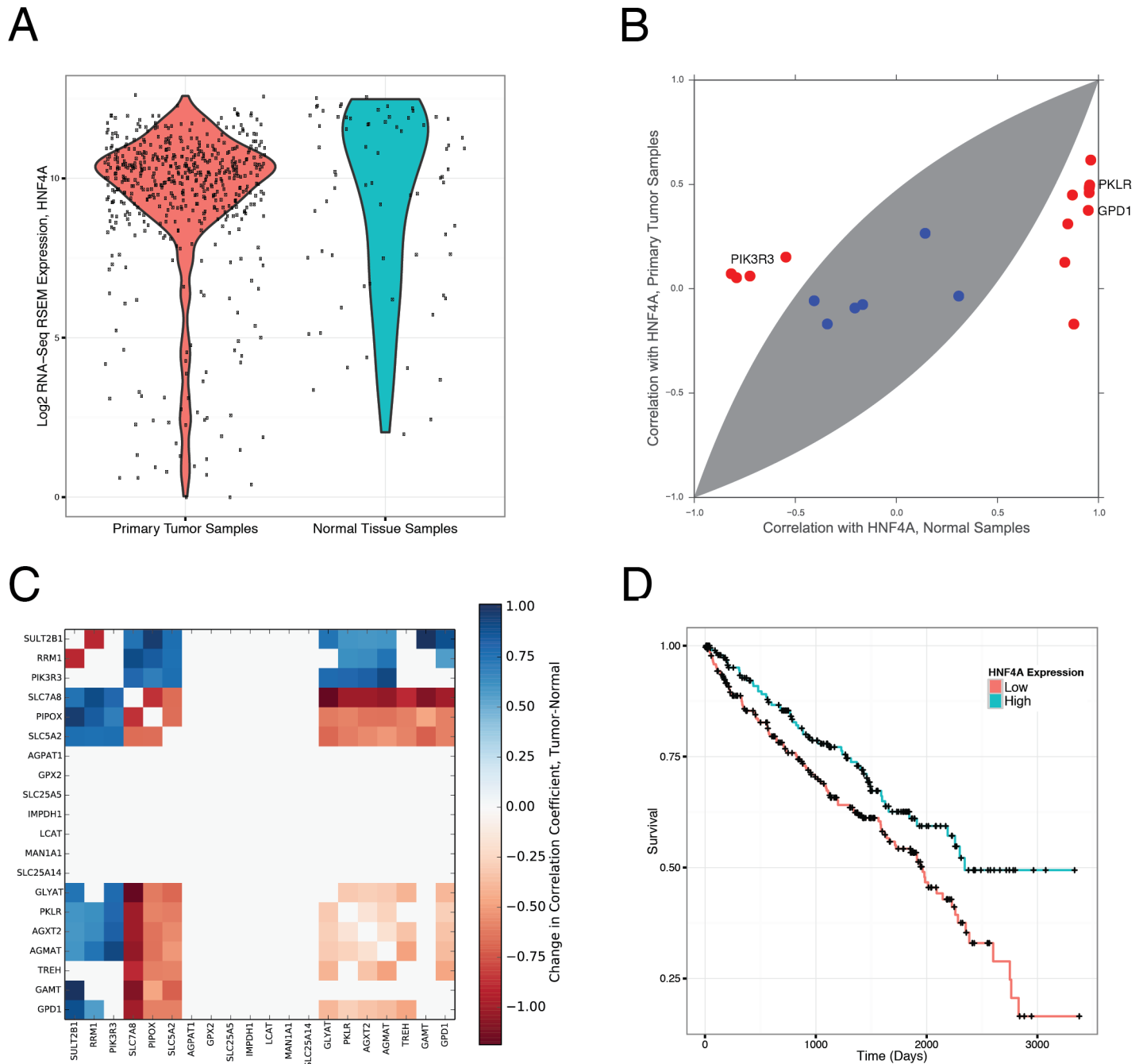


Fig 4. The targets of HNF4A are enriched for differential co-expression in KIRC. (A) HNF4A is not differentially expressed between tumor and adjacent normal tissue samples in KIRC. Each dot corresponds to the expression of HNF4A in one sample of either primary KIRC tumor or normal kidney tissue. (B) Nevertheless, the metabolic gene targets of HNF4A show a distinct loss of co-expression with HNF4A in tumor samples. Several of these genes reside in central carbon metabolism. Genes outside the shaded area correspond to statistically significant instances of differential co-expression. (C) Heatmap of differential co-expression for the 20 metabolic gene targets of HNF4A containing the motif AARGTCCAN around the transcription start site. Value of each square indicates the difference in correlation coefficients between tumor and normal samples, with statistically insignificant differences set to zero. A strict p -value threshold of 1×10^{-4} was used to assign statistical significance. (D) Survival curves for patients showing low or high expression of HNF4A. Patients with low expression of HNF4A exhibited worse outcomes.

doi:10.1371/journal.pcbi.1004176.g004

tumors, we have made little effort to search for common patterns across many different types of tumors. Such a search is necessarily complicated by the fact that our analytical method requires large numbers of normal and tumor samples for sufficient statistical power. The TCGA features few studies with large numbers of normal RNA-Seq samples. In order to balance the need for statistical power with our desire to detect so-called “PanCancer” patterns of differential co-expression, we included five more studies (lung adenocarcinoma, LUAD; hepatocellular carcinoma, LIHC; prostate adenocarcinoma, PRAD; head and neck squamous cell cancer, HNSC; and thyroid cancer, THCA) with at least 30 normal RNA-Seq samples, in our analysis. To increase the confidence of our predictions, we used a stricter p-value threshold of $\tau = 1 \times 10^{-4}$ to call statistically significant differential co-expression.

The results of the PanCan analysis are shown in Fig 5. We retained only those genes which were members of a gene pair which was differentially co-expressed in at least three of the seven studies. Out of the 1789 metabolic genes under study, only 50 genes satisfied this criteria. Interestingly, many of these genes encode key enzymes in central metabolism (for example, PC, pyruvate carboxylase; LDHD, D-lactate dehydrogenase; IDH1, isocitrate dehydrogenase 1; ALDOA, aldolase A), pointing to apparently recurrent dysregulations of core pathways.

Among the many individual results of our PanCan analysis, perhaps the most interesting was the recurrent dysregulation of four genes in the mitochondrial electron transport chain (ETC): two genes associated with mitochondrial ATP synthase complex V (ATP5F1 and ATP5L), COX7B (part of the complex IV cytochrome c oxidase), and NDUFV2 (complex I). A number of other mitochondrial ETC genes are also differentially co-expressed (but to a lesser extent), including UQCR10, UQCRC2, UQCRC1, ATP5A1, and NDUFS3. Given how critical these protein complexes are to energy production and proliferation, we examined in detail the co-expression patterns of ATP5F1 and ATP5L. We found an exceptionally strong correlation in the expression of both genes in normal tissue. Across all seven studies, the expression of both genes was almost precisely equal (Fig 5B, blue dots). However, in tumor samples, the strength of the co-expression (as measured by the correlation coefficient) was substantially weaker. Notably, ATP5F1 and ATP5L were not differentially expressed; instead, their co-expression simply appeared “noisier” in tumor samples. To quantify whether this “noisier” co-expression may be occurring by chance, we fit each co-expression pattern in Fig 5B to a line, and then calculated the variance of the residuals of the fit. We used Levene’s test to test whether the variance of the residuals associated with tumor samples was larger than the variance of the residuals associated with normal samples. In all four tumor types, we confirmed that the tumor samples showed higher variance (p-value 7×10^{-17} , 3×10^{-3} , 6×10^{-9} , 6×10^{-6} , 3×10^{-11} , 2×10^{-3} , 5×10^{-3} for BRCA, HNSC, KIRC, LIHC, LUAD, PRAD, and THAC samples, respectively).

The functional consequences of these increasingly “noisy” co-expression patterns in ATP5F1 and ATP5L are unclear. It is known that stoichiometric imbalances of proteins (for example as a result of changes in gene dosage) in complex with each other can manifest phenotypically [49]. Given the recurrence of differential co-expression of three different gene pairs containing ATP5F1 and a second mitochondrial matrix member (ATP5L, COX7B, and NDUFV2), it is tempting to speculate that differential co-expression of ATP5F1 may lead to an altered mitochondrial phenotype. In particular, an imbalance in the levels of ATP5F1 and ATP5L may cause defects in the ability of mitochondria to efficiently conduct oxidative phosphorylation via the electron transport chain. Further experiments are required to evaluate this hypothesis.

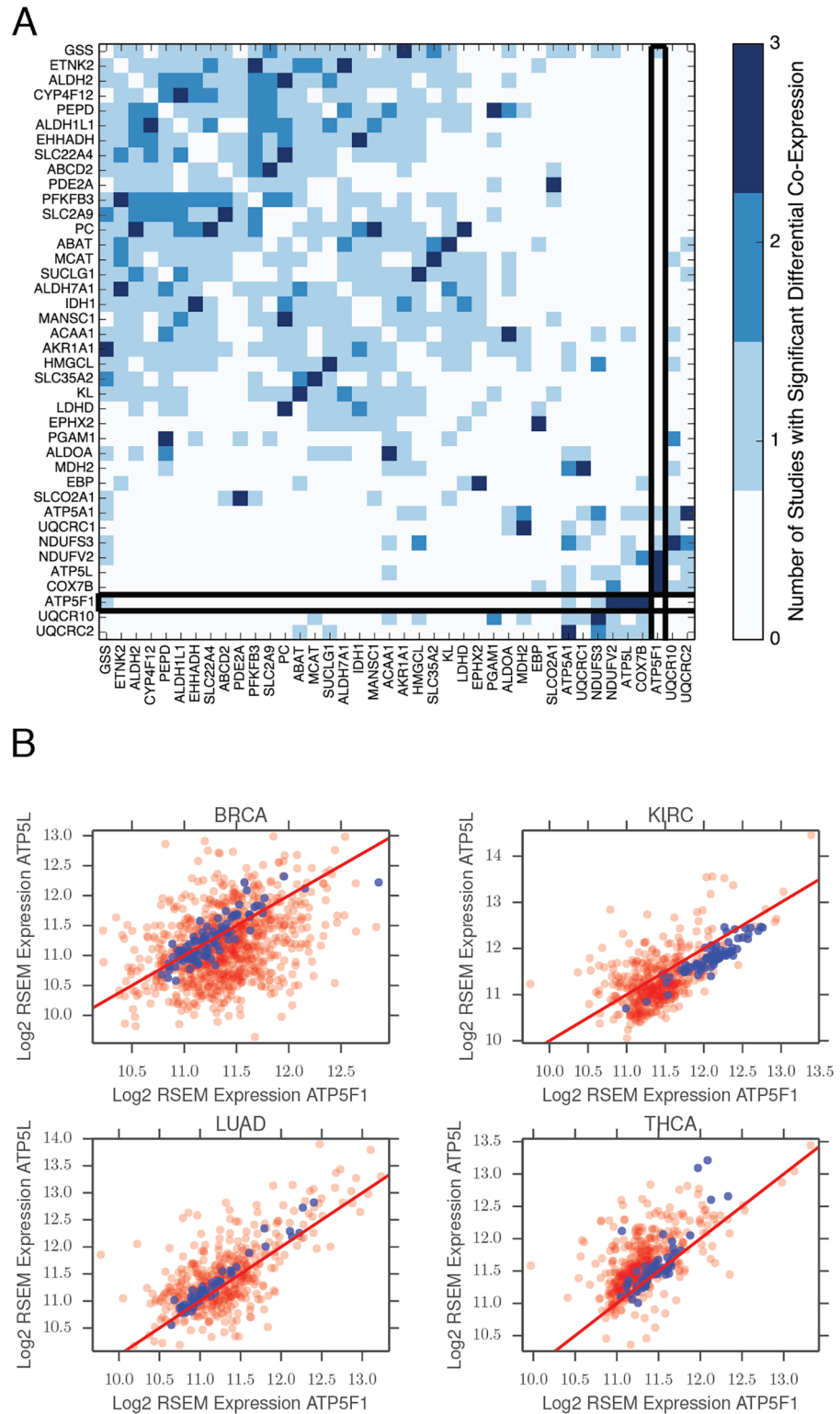


Fig 5. PanCan analysis of differential co-expression. (A) All gene pairs which showed differential co-expression in at least 3 out of 4 different TCGA studies were identified. Approximately 50 unique metabolic genes participated in these recurrently differentially co-expressed pairs. The differential co-expression across all possible pairs of these genes is depicted in the heatmap. A p-value threshold of 1×10^{-4} was used to assign statistical significance for differential co-expression. Special emphasis is placed on ATP5F1. **(B)** Co-

expression of ATP5F1 and ATP5L, both members of mitochondrial Complex V, in four different TCGA studies (blue dots: normal tissue samples; red dots: tumor samples). Red line corresponds to perfect 1:1 correlation. Tumor samples exhibit substantially noisier co-expression of these two genes.

doi:10.1371/journal.pcbi.1004176.g005

Discussion

In this work, we have searched for signals of differential co-expression in tumors. Among our findings, the most relevant is simply the prevalence of differential co-expression throughout metabolism. Gene expression studies are frequently the “first-step” analytical method of choice for understanding the consequences of a perturbation on an organism, or for the comparison of two distinct subsets of samples. While standard methods for differential expression analysis offer useful insights into the differential regulation of genes, our findings here (and the prior findings of others studying differential co-expression) suggest that a great deal of information remains to be culled from the study of “second-order” co-expression patterns between pairs of genes. We have shown that these two measures (differential expression and differential co-expression) are not interchangeable, and in many cases point to distinct regions of the metabolic network that may be dysregulated. Of course, it is important to remember that while the statistical power of both approaches relies on large sample sizes, differential co-expression is significantly more sensitive to sample size upon multiple hypothesis correction because of the large number of independent statistical tests (equal to the square of the number of genes) under evaluation. It will be interesting in the future to compare the results of our work to other methods for calculating differential interactions (*e.g.* partial correlations).

The orthogonality of differential expression and differential co-expression described above suggests that, to detect changes in the activity of a pathway, one must separately investigate the unilateral increase/decrease of enzyme levels, as well changes in their coordinated co-expression. In the first case, the expression of a large set of genes (for example, those in a long, linear metabolic pathway) may be synchronously upregulated. This coordinated up-regulation of transcription may, for example, enable the pathway to carry substantially more metabolic flux. In the second, perhaps more subtle case, the characteristic pattern of flux through a pathway may be re-wired (as illustrated in [Fig 6](#)). In [Fig 6](#), the mechanism for this re-wiring is transcriptional, but in principle this type of coupling may arise through a variety of distinct mechanisms (such as, for example, post-translational modification). In both cases, changes in intra- or extra-cellular conditions across a set of samples induces variation in the expression of genes. However, the manifestation of these changes may be hidden from either differential expression or differential co-expression analysis. Thus, we argue that both differential expression and differential co-expression analysis should play central, complementary roles in the analysis of gene expression data [[11](#)].

Our findings here are a small, first step in applying such a second-order analysis to cancer data, and in particular to the study of cancer metabolism. We have made a number of assumptions in order to make progress in the analysis, and these assumptions should be re-visited in future work. In particular, we have repeatedly assumed that the expression of a gene roughly correlates with the abundance of its translated protein product, and that this abundance correlates with enzyme activity. An entire field of theoretical study (metabolic control analysis, [[50](#)]) and a number of experimental studies (*e.g.* [[51](#)]) have shown that metabolite abundances are equally, if not more, important for the control of fluxes. We note, given an adequately large number of samples, an analogous “differential correlation analysis” is possible for

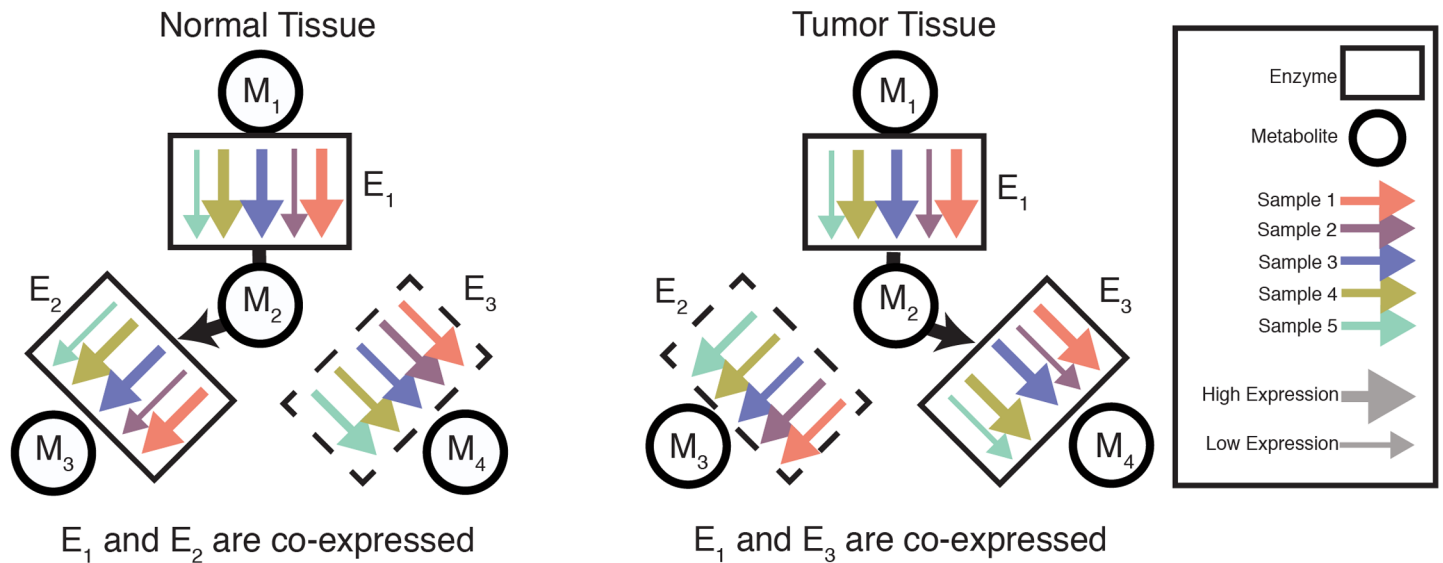


Fig 6. Differential co-expression can signal a change in the activity of a pathway. Each arrow represents the level of expression of an enzymatic gene from a single sample (e.g. a patient, so that all arrows of the same color derive from the same sample). In normal tissue, the expression of genes encoding enzymes E_1 and E_2 are strongly correlated, and the expression of E_1 and E_3 are uncorrelated. In tumor tissue, the expression of genes encoding enzymes E_1 and E_3 are strongly correlated, and the expression of E_1 and E_2 are uncorrelated. If we assume that enzyme activity is correlated with expression, then we may hypothesize that the metabolic flux exiting from E_1 is coupled to flux in E_2 in normal tissue, and to flux in E_3 in tumor tissue. Note that the average expression of these genes remains constant between tumor and normal conditions, so that a differential expression analysis would be unlikely to identify the expression of these genes as anomalous.

doi:10.1371/journal.pcbi.1004176.g006

metabolomics data. It would be especially interesting to compare the results from such an analysis with the analogous results using expression data.

One major concern with our results are the confounding effects of (1) contamination by stromal and immune cells, and (2) existence of heterogeneous tumor subtypes in the data. Tumor samples are often contaminated with mixtures of normal adjacent tissue and immune cells. Deconvolving the contribution of non-cancerous cells from the total signal obtained from a tumor sample remains a major computational challenge, and it is unclear how the contribution of this non-cancerous signal affects our differential co-expression results. A separate but related concern is the existence of distinct molecular subtypes in a set of samples (e.g. ER^+ , ER^- breast cancer samples). We have not made any efforts to tease apart the confounding effects of these distinct subtypes in our work. Interestingly, it is possible that a significant portion of the differential co-expression signal we identify derives directly from these subtypes; in other words, the primary differences between subtypes may lie among the differentially co-expressed genes. Evaluating such a hypothesis will require substantially larger sample sizes. Nevertheless, we feel that a more careful analysis of such patterns after subtype separation and stromal deconvolution is a lucrative route for future studies.

Finally, we would like to comment on the complementarity of differential expression and co-expression which we have proposed. In the course of responding to environmental stresses and stresses, it is inevitable that some genes will be both differentially expressed as well as differentially co-expressed. We are not arguing that one measure is superior to the other; rather, each offers a different glimpse onto the response of a highly-connected network to a perturbation. Neither the over-expression of a single gene, nor an increase in the co-expression of a pair of genes, signals a change in a pathway's activity. However, by monitoring both measures, one

univariate and the other multivariate, one may obtain a more complete picture of the complex system under examination.

Supporting Information

S1 Code. Python function for the differential co-expression statistical test.

(PY)

S1 Fig. A comparison of the difference in correlation coefficient in clear cell kidney cancer for the true (red) and permuted random (purple) data sets. The labels (*i.e.* tumor or normal) of all RNA-Seq samples were permuted, and the difference in correlation coefficient calculated. This process was repeated 10000 times to generate a distribution. Differences in correlation coefficients tend to be larger in the true data, suggesting that differential co-expression is being observed.

(PDF)

S2 Fig. Comparison of changes in Spearman correlation coefficient for functionally related genes in BRCA. In top panel, a comparison is made between gene pairs whose products are in complex with each other, and gene pairs whose products are not in complex with each other. In the bottom panel, the unit of interaction is the “catalysis-precedes” binary interaction in Pathway Commons. A gene pair participates in this interaction if the gene products share a common substrate or product. Note that from the top panel, gene pairs whose products are members of a common complex show loss of co-expression in tumor samples.

(PDF)

S3 Fig. Comparison of changes in Spearman correlation coefficient for functionally related genes in KIRC. In top panel, a comparison is made between gene pairs whose products are in complex with each other, and gene pairs whose products are not in complex with each other. In the bottom panel, the unit of interaction is the “catalysis-precedes” binary interaction in Pathway Commons. A gene pair participates in this interaction if the gene products share a common substrate or product. Note that from the top panel, gene pairs whose products are members of a common complex show loss of co-expression in tumor samples.

(PDF)

S4 Fig. Differential co-expression in PSAT1 in KIRC. Blue dots correspond to normal tissue samples and red dots correspond to tumor samples.

(PDF)

S5 Fig. Novel co-expression in KIRC tumors with PSAT1. Blue dots correspond to normal tissue samples and red dots correspond to tumor samples.

(PDF)

S6 Fig. Differential co-expression in ACAT1 in BRCA. Blue dots correspond to normal tissue samples and red dots correspond to tumor samples.

(PDF)

S7 Fig. Differential expression and differential co-expression are only weakly correlated. X-axis corresponds to the absolute value of the \log_2 ratio of expression between tumor and normal tissues.

(PDF)

S8 Fig. Differential co-expression of HNF4 with its metabolic gene targets in KIRC. Blue dots correspond to normal tissue samples and red dots correspond to tumor samples.

(PDF)

Acknowledgments

We gratefully acknowledge B. Arman Aksoy for assistance on the identification of molecular complexes.

Author Contributions

Analyzed the data: ER. Wrote the paper: ER CS.

References

1. Koppenol WH, Bounds PL, Dang CV. Otto Warburg's contributions to current concepts of cancer metabolism. *Nature reviews Cancer*. 2011 May; 11(5):325–37. Available from: <http://dx.doi.org/10.1038/nrc3038>. doi: [10.1038/nrc3038](https://doi.org/10.1038/nrc3038) PMID: [21508971](https://pubmed.ncbi.nlm.nih.gov/21508971/)
2. Ye J, Mancuso A, Tong X, Ward PS, Fan J, Rabinowitz JD, et al. Pyruvate kinase M2 promotes de novo serine synthesis to sustain mTORC1 activity and cell proliferation. *Proceedings of the National Academy of Sciences of the United States of America*. 2012 May; 109(18):6904–9. Available from: <http://www.pnas.org/content/early/2012/04/10/1204176109>. doi: [10.1073/pnas.1204176109](https://doi.org/10.1073/pnas.1204176109) PMID: [22509023](https://pubmed.ncbi.nlm.nih.gov/22509023/)
3. Lu C, Ward PS, Kapoor GS, Rohle D, Turcan S, Abdel-Wahab O, et al. IDH mutation impairs histone demethylation and results in a block to cell differentiation. *Nature*. 2012 Mar; 483(7390):474–8. Available from: <http://www.pubmedcentral.nih.gov/articlerender.fcgi?artid=3478770&tool=pmcentrez&rendertype=abstract>. doi: [10.1038/nature10860](https://doi.org/10.1038/nature10860) PMID: [22343901](https://pubmed.ncbi.nlm.nih.gov/22343901/)
4. Wang HQ, Tsai CJ. CorSig: a general framework for estimating statistical significance of correlation and its application to gene co-expression analysis. *PloS one*. 2013 Jan; 8(10):e77429. Available from: <http://dx.plos.org/10.1371/journal.pone.0077429>. doi: [10.1371/journal.pone.0077429](https://doi.org/10.1371/journal.pone.0077429) PMID: [24194884](https://pubmed.ncbi.nlm.nih.gov/24194884/)
5. Rhinn H, Fujita R, Qiang L, Cheng R, Lee JH, Abeliovich A. Integrative genomics identifies APOE ε4 effectors in Alzheimer's disease. *Nature*. 2013 Aug; 500(7460):45–50. Available from: <http://www.nature.com/nature/journal/v500/n7460/full/nature12415.html#ref18>. doi: [10.1038/nature12415](https://doi.org/10.1038/nature12415) PMID: [23883936](https://pubmed.ncbi.nlm.nih.gov/23883936/)
6. Fang G, Kuang R, Pandey G, Steinbach M, Myers CL, Kumar V. Subspace differential coexpression analysis: problem definition and a general approach. *Pacific Symposium on Biocomputing Pacific Symposium on Biocomputing*. 2010 Jan;p. 145–56. Available from: <http://www.ncbi.nlm.nih.gov/pubmed/19908367>. PMID: [19908367](https://pubmed.ncbi.nlm.nih.gov/19908367/)
7. Chiang JH, Chang TH, Kao HY, Fukushima A. DiffCorr: An R package to analyze and visualize differential correlations in biological networks. *Gene*. 2013; 518(1):209–214. Available from: <http://www.sciencedirect.com/science/article/pii/S0378111912014497>. doi: [10.1016/j.gene.2012.11.028](https://doi.org/10.1016/j.gene.2012.11.028)
8. Ihmels J, Bergmann S, Berman J, Barkai N. Comparative gene expression analysis by differential clustering approach: application to the *Candida albicans* transcription program. *PLoS genetics*. 2005 Sep; 1(3):e39. Available from: <http://www.pubmedcentral.nih.gov/articlerender.fcgi?artid=1239936&tool=pmcentrez&rendertype=abstract>. doi: [10.1371/journal.pgen.0010039](https://doi.org/10.1371/journal.pgen.0010039) PMID: [16470937](https://pubmed.ncbi.nlm.nih.gov/16470937/)
9. Choi JK, Yu U, Yoo OJ, Kim S. Differential coexpression analysis using microarray data and its application to human cancer. *Bioinformatics (Oxford, England)*. 2005 Dec; 21(24):4348–55. Available from: <http://bioinformatics.oxfordjournals.org/content/21/24/4348>. doi: [10.1093/bioinformatics/bti722](https://doi.org/10.1093/bioinformatics/bti722)
10. Liu BH, Yu H, Tu K, Li C, Li YX, Li YY. DCGL: an R package for identifying differentially coexpressed genes and links from gene expression microarray data. *Bioinformatics (Oxford, England)*. 2010 Oct; 26(20):2637–8. Available from: <http://www.pubmedcentral.nih.gov/articlerender.fcgi?artid=2951087&tool=pmcentrez&rendertype=abstract>. doi: [10.1093/bioinformatics/btq471](https://doi.org/10.1093/bioinformatics/btq471)
11. Ideker T, Krogan NJ. Differential network biology. *Molecular systems biology*. 2012 Jan; 8(1):565. Available from: <http://msb.embopress.org/content/8/1/565.abstract>. doi: [10.1038/msb.2011.99](https://doi.org/10.1038/msb.2011.99) PMID: [22252388](https://pubmed.ncbi.nlm.nih.gov/22252388/)
12. Hu J, Locasale JW, Bielas JH, O'Sullivan J, Sheahan K, Cantley LC, et al. Heterogeneity of tumor-induced gene expression changes in the human metabolic network. *Nature biotechnology*. 2013 Jun; 31(6):522–9. Available from: <http://dx.doi.org/10.1038/nbt.2530>. doi: [10.1038/nbt.2530](https://doi.org/10.1038/nbt.2530) PMID: [23604282](https://pubmed.ncbi.nlm.nih.gov/23604282/)
13. Nilsson R, Jain M, Madhusudhan N, Sheppard NG, Strittmatter L, Kampf C, et al. Metabolic enzyme expression highlights a key role for MTHFD2 and the mitochondrial folate pathway in cancer. *Nature communications*. 2014 Jan; 5:3128. Available from: <http://www.nature.com/ncomms/2014/140123/ncomms4128/full/ncomms4128.html>. doi: [10.1038/ncomms4128](https://doi.org/10.1038/ncomms4128) PMID: [24451681](https://pubmed.ncbi.nlm.nih.gov/24451681/)

14. Lai Y, Wu B, Chen L, Zhao H. A statistical method for identifying differential gene-gene co-expression patterns. *Bioinformatics* (Oxford, England). 2004 Nov; 20(17):3146–55. Available from: <http://bioinformatics.oxfordjournals.org/content/20/17/3146.short>. doi: [10.1093/bioinformatics/bth379](https://doi.org/10.1093/bioinformatics/bth379)
15. Carter SL, Brechbühler CM, Griffin M, Bond AT. Gene co-expression network topology provides a framework for molecular characterization of cellular state. *Bioinformatics* (Oxford, England). 2004 Sep; 20(14):2242–50. Available from: <http://bioinformatics.oxfordjournals.org/content/20/14/2242>. doi: [10.1093/bioinformatics/bth234](https://doi.org/10.1093/bioinformatics/bth234)
16. Bockmayr M, Klauschen F, Györfy B, Denkert C, Budczies J. New network topology approaches reveal differential correlation patterns in breast cancer. *BMC systems biology*. 2013 Jan; 7:78. Available from: <http://www.pubmedcentral.nih.gov/articlerender.fcgi?artid=3848818&tool=pmcentrez&rendertype=abstract>. doi: [10.1186/1752-0509-7-78](https://doi.org/10.1186/1752-0509-7-78) PMID: [23945349](https://pubmed.ncbi.nlm.nih.gov/23945349/)
17. Amar D, Safer H, Shamir R. Dissection of regulatory networks that are altered in disease via differential co-expression. *PLoS computational biology*. 2013 Jan; 9(3):e1002955. Available from: <http://www.pubmedcentral.nih.gov/articlerender.fcgi?artid=3591264&tool=pmcentrez&rendertype=abstract>. doi: [10.1371/journal.pcbi.1002955](https://doi.org/10.1371/journal.pcbi.1002955) PMID: [23505361](https://pubmed.ncbi.nlm.nih.gov/23505361/)
18. Hudson NJ, Reverter A, Dalrymple BP. A differential wiring analysis of expression data correctly identifies the gene containing the causal mutation. *PLoS computational biology*. 2009 May; 5(5):e1000382. Available from: <http://dx.plos.org/10.1371/journal.pcbi.1000382>. doi: [10.1371/journal.pcbi.1000382](https://doi.org/10.1371/journal.pcbi.1000382) PMID: [19412532](https://pubmed.ncbi.nlm.nih.gov/19412532/)
19. Thiele I, Swainston N, Fleming RMT, Hoppe A, Sahoo S, Aurich MK, et al. A community-driven global reconstruction of human metabolism. *Nature biotechnology*. 2013 May; 31(5):419–25. Available from: <http://dx.doi.org/10.1038/nbt.2488>. doi: [10.1038/nbt.2488](https://doi.org/10.1038/nbt.2488) PMID: [23455439](https://pubmed.ncbi.nlm.nih.gov/23455439/)
20. Dudoit S, Schaffer J, Boldrick J. Multiple hypothesis testing in microarray experiments. *Statistical Science*. 2003; 18(1):71–103. doi: [10.1214/ss/1056397487](https://doi.org/10.1214/ss/1056397487)
21. Fisher RA. On the “Probable Error” of a Coefficient of Correlation Deduced from a Small Sample. *Metron*. 1921; 1:3–32. Available from: <http://digital.library.adelaide.edu.au/dspace/handle/2440/15169>.
22. Kenny DA. *Statistics for the Social and Behavioral Sciences*. Little, Brown; 1987.
23. Liberzon A, Subramanian A, Pinchback R, Thorvaldsdóttir H, Tamayo P, Mesirov JP. Molecular signatures database (MSigDB) 3.0. *Bioinformatics* (Oxford, England). 2011 Jun; 27(12):1739–40. Available from: <http://bioinformatics.oxfordjournals.org/content/27/12/1739.short>. doi: [10.1093/bioinformatics/btr260](https://doi.org/10.1093/bioinformatics/btr260)
24. Won S, Morris N, Lu Q, Elston RC. Choosing an optimal method to combine P-values. *Statistics in medicine*. 2009 May; 28(11):1537–53. Available from: <http://www.pubmedcentral.nih.gov/articlerender.fcgi?artid=2771157&tool=pmcentrez&rendertype=abstract> doi: [10.1002/sim.3569](https://doi.org/10.1002/sim.3569) PMID: [19266501](https://pubmed.ncbi.nlm.nih.gov/19266501/).
25. Freed-Pastor WA, Mizuno H, Zhao X, Langerød A, Moon SH, Rodriguez-Barrueco R, et al. Mutant p53 disrupts mammary tissue architecture via the mevalonate pathway. *Cell*. 2012 Jan; 148(1–2):244–58. Available from: [http://www.cell.com/fulltext/S0092-8674\(11\)01569-8](http://www.cell.com/fulltext/S0092-8674(11)01569-8). doi: [10.1016/j.cell.2011.12.017](https://doi.org/10.1016/j.cell.2011.12.017) PMID: [22265415](https://pubmed.ncbi.nlm.nih.gov/22265415/)
26. Clendening JW, Pandeyra A, Boutros PC, El Ghamrasni S, Khosravi F, Trentin GA, et al. Dysregulation of the mevalonate pathway promotes transformation. *Proceedings of the National Academy of Sciences of the United States of America*. 2010 Aug; 107(34):15051–6. Available from: <http://www.pnas.org/content/107/34/15051.long>. doi: [10.1073/pnas.0910258107](https://doi.org/10.1073/pnas.0910258107) PMID: [20696928](https://pubmed.ncbi.nlm.nih.gov/20696928/)
27. Possemato R, Marks KM, Shaul YD, Pacold ME, Kim D, Birsoy K, et al. Functional genomics reveal that the serine synthesis pathway is essential in breast cancer. *Nature*. 2011 Aug; 476(7360):346–50. Available from: <http://dx.doi.org/10.1038/nature10350>. doi: [10.1038/nature10350](https://doi.org/10.1038/nature10350) PMID: [21760589](https://pubmed.ncbi.nlm.nih.gov/21760589/)
28. Vié N, Copois V, Bascoul-Mollevi C, Denis V, Bec N, Robert B, et al. Overexpression of phosphoserine aminotransferase PSAT1 stimulates cell growth and increases chemoresistance of colon cancer cells. *Molecular cancer*. 2008 Jan; 7(1):14. Available from: <http://www.molecular-cancer.com/content/7/1/14>. doi: [10.1186/1476-4598-7-14](https://doi.org/10.1186/1476-4598-7-14) PMID: [18221502](https://pubmed.ncbi.nlm.nih.gov/18221502/)
29. Delage B, Fennell DA, Nicholson L, McNeish I, Lemoine NR, Crook T, et al. Arginine deprivation and argininosuccinate synthetase expression in the treatment of cancer. *International journal of cancer Journal international du cancer*. 2010 Jun; 126(12):2762–72. Available from: <http://www.ncbi.nlm.nih.gov/pubmed/20104527>. PMID: [20104527](https://pubmed.ncbi.nlm.nih.gov/20104527/)
30. Qiu F, Chen YR, Liu X, Chu CY, Shen LJ, Xu J, et al. Arginine Starvation Impairs Mitochondrial Respiratory Function in ASS1-Deficient Breast Cancer Cells. *Science Signaling*. 2014 Apr; 7(319):ra31–ra31. Available from: <http://stke.sciencemag.org/cgi/content/abstract/7/319/ra31>. doi: [10.1126/scisignal.2004761](https://doi.org/10.1126/scisignal.2004761) PMID: [24692592](https://pubmed.ncbi.nlm.nih.gov/24692592/)

31. Jeschke J, O'Hagan HM, Zhang W, Vatapalli R, Calmon MF, Danilova L, et al. Frequent inactivation of cysteine dioxygenase type 1 contributes to survival of breast cancer cells and resistance to anthracyclines. *Clinical cancer research: an official journal of the American Association for Cancer Research*. 2013 Jun; 19(12):3201–11. Available from: <http://www.ncbi.nlm.nih.gov/pubmed/23630167>. doi: [10.1158/1078-0432.CCR-12-3751](https://doi.org/10.1158/1078-0432.CCR-12-3751)
32. Denkert C, Bucher E, Hilvo M, Salek R, Orešič M, Griffin J, et al. Metabolomics of human breast cancer: new approaches for tumor typing and biomarker discovery. *Genome medicine*. 2012 Jan; 4(4):37. Available from: <http://genomemedicine.com/content/4/4/37>. doi: [10.1186/gm336](https://doi.org/10.1186/gm336) PMID: [22546809](https://pubmed.ncbi.nlm.nih.gov/22546809/)
33. Nomura DK, Long JZ, Niessen S, Hoover HS, Ng SW, Cravatt BF. Monoacylglycerol lipase regulates a fatty acid network that promotes cancer pathogenesis. *Cell*. 2010 Jan; 140(1):49–61. Available from: <http://www.sciencedirect.com/science/article/pii/S0092867409014391>. doi: [10.1016/j.cell.2009.11.027](https://doi.org/10.1016/j.cell.2009.11.027) PMID: [20079333](https://pubmed.ncbi.nlm.nih.gov/20079333/)
34. Cerami EG, Gross BE, Demir E, Rodchenkov I, Babur O, Anwar N, et al. Pathway Commons, a web resource for biological pathway data. *Nucleic acids research*. 2011 Jan; 39(Database issue):D685–90. Available from: http://nar.oxfordjournals.org/content/39/suppl_1/D685.short. doi: [10.1093/nar/gkq1039](https://doi.org/10.1093/nar/gkq1039) PMID: [21071392](https://pubmed.ncbi.nlm.nih.gov/21071392/)
35. Babur O, Aksoy BA, Rodchenkov I, Sümer SO, Sander C, Demir E. Pattern search in BioPAX models. *Bioinformatics (Oxford, England)*. 2014 Jan; 30(1):139–40. Available from: <http://bioinformatics.oxfordjournals.org/content/30/1/139.full>. doi: [10.1093/bioinformatics/btt539](https://doi.org/10.1093/bioinformatics/btt539)
36. Hlaváč V, Brynychová V, Václavíková R, Ehrlichová M, Vrána D, Pecha V, et al. The expression profile of ATP-binding cassette transporter genes in breast carcinoma. *Pharmacogenomics*. 2013 Apr; 14(5):515–29. Available from: <http://www.ncbi.nlm.nih.gov/pubmed/23556449>. doi: [10.2217/pgs.13.26](https://doi.org/10.2217/pgs.13.26) PMID: [23556449](https://pubmed.ncbi.nlm.nih.gov/23556449/)
37. Law CW, Chen Y, Shi W, Smyth GK. Voom: precision weights unlock linear model analysis tools for RNA-seq read counts. *Genome biology*. 2014 Feb; 15(2):R29. Available from: <http://genomebiology.com/2014/15/2/R29>. doi: [10.1186/gb-2014-15-2-r29](https://doi.org/10.1186/gb-2014-15-2-r29) PMID: [24485249](https://pubmed.ncbi.nlm.nih.gov/24485249/)
38. Gilkes DM, Bajpai S, Wong CC, Chaturvedi P, Hubbi ME, Wirtz D, et al. Procollagen lysyl hydroxylase 2 is essential for hypoxia-induced breast cancer metastasis. *Molecular cancer research: MCR*. 2013 May; 11(5):456–66. Available from: <http://www.ncbi.nlm.nih.gov/pubmed/23378577>. doi: [10.1158/1541-7786.MCR-12-0629](https://doi.org/10.1158/1541-7786.MCR-12-0629) PMID: [23378577](https://pubmed.ncbi.nlm.nih.gov/23378577/)
39. Almaraz RT, Tian Y, Bhattacharya R, Tan E, Chen SH, Dallas MR, et al. Metabolic flux increases glycoprotein sialylation: implications for cell adhesion and cancer metastasis. *Molecular & cellular proteomics: MCP*. 2012 Jul; 11(7):M112.017558. Available from: <http://www.pubmedcentral.nih.gov/articlerender.fcgi?artid=3394959&tool=pmcentrez&rendertype=abstract>. doi: [10.1074/mcp.M112.017558](https://doi.org/10.1074/mcp.M112.017558)
40. Reverter A, Hudson NJ, Nagaraj SH, Pérez-Enciso M, Dalrymple BP. Regulatory impact factors: unraveling the transcriptional regulation of complex traits from expression data. *Bioinformatics (Oxford, England)*. 2010 Apr; 26(7):896–904. Available from: <http://bioinformatics.oxfordjournals.org/content/26/7/896.html>. doi: [10.1093/bioinformatics/btq051](https://doi.org/10.1093/bioinformatics/btq051)
41. Li L, Davie JR. The role of Sp1 and Sp3 in normal and cancer cell biology. *Annals of anatomy = Anatomischer Anzeiger: official organ of the Anatomische Gesellschaft*. 2010 Sep; 192(5):275–83. Available from: <http://www.ncbi.nlm.nih.gov/pubmed/20810260>. doi: [10.1016/j.aanat.2010.07.010](https://doi.org/10.1016/j.aanat.2010.07.010)
42. Chuang CW, Pan MR, Hou MF, Hung WC. Cyclooxygenase-2 up-regulates CCR7 expression via AKT-mediated phosphorylation and activation of Sp1 in breast cancer cells. *Journal of cellular physiology*. 2013 Feb; 228(2):341–8. Available from: <http://www.ncbi.nlm.nih.gov/pubmed/22718198>. doi: [10.1002/jcp.24136](https://doi.org/10.1002/jcp.24136) PMID: [22718198](https://pubmed.ncbi.nlm.nih.gov/22718198/)
43. Yiu GK, Toker A. NFAT induces breast cancer cell invasion by promoting the induction of cyclooxygenase-2. *The Journal of biological chemistry*. 2006 May; 281(18):12210–7. Available from: <http://www.jbc.org/content/281/18/12210.short>. doi: [10.1074/jbc.M600184200](https://doi.org/10.1074/jbc.M600184200) PMID: [16505480](https://pubmed.ncbi.nlm.nih.gov/16505480/)
44. Ariazi EA, Kraus RJ, Farrell ML, Jordan VC, Mertz JE. Estrogen-related receptor alpha1 transcriptional activities are regulated in part via the ErbB2/HER2 signaling pathway. *Molecular cancer research: MCR*. 2007 Jan; 5(1):71–85. Available from: <http://www.ncbi.nlm.nih.gov/pubmed/17259347>. doi: [10.1158/1541-7786.MCR-06-0227](https://doi.org/10.1158/1541-7786.MCR-06-0227) PMID: [17259347](https://pubmed.ncbi.nlm.nih.gov/17259347/)
45. Ariazi EA, Clark GM, Mertz JE. Estrogen-related receptor alpha and estrogen-related receptor gamma associate with unfavorable and favorable biomarkers, respectively, in human breast cancer. *Cancer research*. 2002 Nov; 62(22):6510–8. Available from: <http://www.ncbi.nlm.nih.gov/pubmed/12438245>. PMID: [12438245](https://pubmed.ncbi.nlm.nih.gov/12438245/)
46. Grigo K, Wirsing A, Lucas B, Klein-Hitpass L, Ryffel GU. HNF4 alpha orchestrates a set of 14 genes to down-regulate cell proliferation in kidney cells. *Biological chemistry*. 2008 Feb; 389(2):179–87. Available from: <http://www.ncbi.nlm.nih.gov/pubmed/18163890>. doi: [10.1515/BC.2008.011](https://doi.org/10.1515/BC.2008.011) PMID: [18163890](https://pubmed.ncbi.nlm.nih.gov/18163890/)

47. Sel S, Ebert T, Ryffel GU, Drewes T. Human renal cell carcinogenesis is accompanied by a coordinate loss of the tissue specific transcription factors HNF4 α and HNF1 α . *Cancer Letters*. 1996 Mar; 101(2):205–210. Available from: <http://www.sciencedirect.com/science/article/pii/0304383596041365>. doi: [10.1016/0304-3835\(96\)04136-5](https://doi.org/10.1016/0304-3835(96)04136-5) PMID: [8620471](https://pubmed.ncbi.nlm.nih.gov/8620471/)
48. Lucas B, Grigo K, Erdmann S, Lausen J, Klein-Hitpass L, Ryffel GU. HNF4 α reduces proliferation of kidney cells and affects genes deregulated in renal cell carcinoma. *Oncogene*. 2005 Sep; 24(42):6418–31. Available from: <http://dx.doi.org/10.1038/sj.onc.1208794>. PMID: [16007190](https://pubmed.ncbi.nlm.nih.gov/16007190/)
49. Veitia RA, Bottani S, Birchler JA. Cellular reactions to gene dosage imbalance: genomic, transcriptomic and proteomic effects. *Trends in genetics: TIG*. 2008 Aug; 24(8):390–7. Available from: <http://www.cell.com/article/S0168952508001741/fulltext>. doi: [10.1016/j.tig.2008.05.005](https://doi.org/10.1016/j.tig.2008.05.005) PMID: [18585818](https://pubmed.ncbi.nlm.nih.gov/18585818/)
50. Fell DA. Metabolic control analysis: a survey of its theoretical and experimental development. *The Biochemical journal*. 1992 Sep; 286 (Pt 2):313–30. Available from: <http://www.pubmedcentral.nih.gov/articlerender.fcgi?artid=1132899&tool=pmcentrez&rendertype=abstract>. PMID: [1530563](https://pubmed.ncbi.nlm.nih.gov/1530563/)
51. Chubukov V, Uhr M, Le Chat L, Kleijn RJ, Jules M, Link H, et al. Transcriptional regulation is insufficient to explain substrate-induced flux changes in *Bacillus subtilis*. *Molecular systems biology*. 2013 Jan; 9:709. Available from: <http://www.ncbi.nlm.nih.gov/pubmed/24281055>. doi: [10.1038/msb.2013.66](https://doi.org/10.1038/msb.2013.66) PMID: [24281055](https://pubmed.ncbi.nlm.nih.gov/24281055/)